

## Accepted Manuscript

Title: Oxidative coupling of methane on cordierite monoliths coated with Sr/La<sub>2</sub>O<sub>3</sub> catalysts. Influence of honeycomb structure and catalyst-cordierite chemical interactions on the catalytic behavior

Authors: Brenda M. Sollier, Leticia E. Gómez, Alicia V. Boix, Eduardo E. Miró

PII: S0926-860X(17)30520-3  
DOI: <https://doi.org/10.1016/j.apcata.2017.10.023>  
Reference: APCATA 16460

To appear in: *Applied Catalysis A: General*

Received date: 21-7-2017  
Revised date: 26-10-2017  
Accepted date: 31-10-2017

Please cite this article as: Brenda M.Sollier, Leticia E.Gómez, Alicia V.Boix, Eduardo E.Miró, Oxidative coupling of methane on cordierite monoliths coated with Sr/La<sub>2</sub>O<sub>3</sub> catalysts.Influence of honeycomb structure and catalyst-cordierite chemical interactions on the catalytic behavior, Applied Catalysis A, General <https://doi.org/10.1016/j.apcata.2017.10.023>

This is a PDF file of an unedited manuscript that has been accepted for publication. As a service to our customers we are providing this early version of the manuscript. The manuscript will undergo copyediting, typesetting, and review of the resulting proof before it is published in its final form. Please note that during the production process errors may be discovered which could affect the content, and all legal disclaimers that apply to the journal pertain.



**Oxidative coupling of methane on cordierite monoliths coated with Sr/La<sub>2</sub>O<sub>3</sub> catalysts. Influence of honeycomb structure and catalyst-cordierite chemical interactions on the catalytic behavior.**

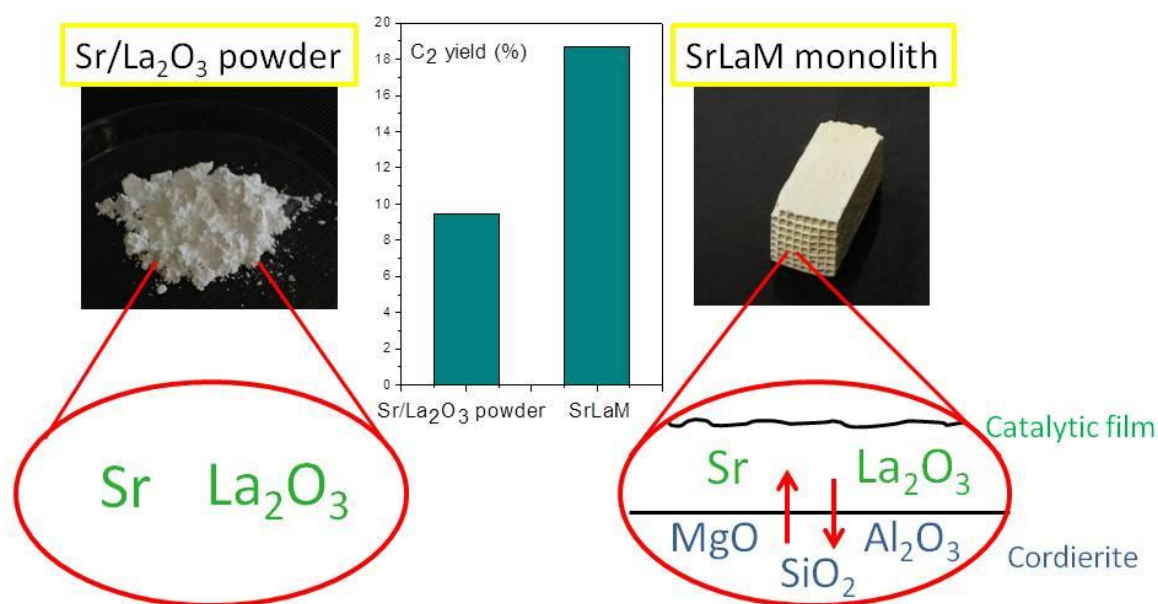
Brenda M. Sollier, Leticia E. Gómez, Alicia V. Boix, Eduardo E. Miró\*

*Instituto de Investigaciones en Catálisis y Petroquímica, INCAPE, Universidad Nacional del Litoral, CONICET, Facultad de Ingeniería Química, Santiago del Estero, 2829-3000 Santa Fe, Argentina*

\* emiro@fiq.unl.edu.ar

Submitted to Applied Catalysis A: General.

Graphical Abstract



Highlights

- Ceramic structures like honeycomb monoliths represent attractive alternatives for their application in real systems.
- The use of structured catalysts results in an important increase of  $C_2$  yield in the oxidative coupling of methane over Sr/La<sub>2</sub>O<sub>3</sub> catalysts.
- The improved catalytic behavior is due to a combination of physical and chemical factors.
- It is suggested that honeycomb structure provides an even flow and an improved mass transfer as compared with the powder catalyst.
- Chemical interactions between the catalytic film and the cordierite material, originated in the incorporation of Mg and Si into the Sr/La<sub>2</sub>O<sub>3</sub> film, promotes methane conversion and  $C_2$  yield.

**Abstract**

When powder Sr/La<sub>2</sub>O<sub>3</sub> catalysts are deposited on the walls of cordierite monoliths, an important increase in both, methane conversion and C<sub>2</sub> yield, takes place. In this work, it is shown that this improved catalytic behavior is due to a combination of physical and chemical factors. This conclusion was drawn after performing a systematic study in which several structured formulations were catalytically evaluated and characterized using different techniques (EDX, XRD, BET, XPS, LRS), which helped us to rationalize the experimental observations. It is suggested that the honeycomb structure provides a more homogeneous gaseous flow as compared with the powder catalyst. This fact results in a better contact between reactant and catalyst surface, which in turn results in an increase of the overall reaction rate. Furthermore, it is demonstrated that the catalytic layer enrichment with Mg and Si, coming from the cordierite structure, greatly contributes to the improved catalytic behavior.

**Keywords:** Methane coupling; Ethane and Ethylene; Monolithic catalyst; Sr/La<sub>2</sub>O<sub>3</sub>.

## 1. Introduction

Natural gas production is expected to expand dramatically in the next few years [1]. Advances in exploration and development of new extracting methods have made it possible to reach to shale deposits previously deemed uneconomical to exploit. One of the biggest natural gas supplies is located in Argentina. According to the latest studies performed in Vaca Muerta region, these deposits would have a potential similar to that of the most productive deposits across the globe [2]. The second biggest natural shale gas reserve and the fourth largest petroleum reserve in the world are located in this region.

Therefore, special interest exists in the opportunity of using these natural supplies and exploiting them to their maximum potential. Today, due to difficulties in transportation, natural gas has been used as a commodity or wasted in the oil wells, causing profound environmental damage. Moreover, methane (main natural gas component) is a greenhouse gas with a global warming potential 20 times that of CO<sub>2</sub> [3].

The abundance of natural gas, the need for its transportation, and environmental concerns are factors that challenge researchers to find and develop better ways of exploiting this resource. Therefore, the conversion of methane into ethane and ethylene via the oxidative coupling of methane (OCM) is an attractive alternative [4,5]. This reaction enables obtaining more valuable products like chemicals or fuels.

The development of the OCM technology is performed by Siluria Technologies. The aim of this company is to reduce costs, energy and environmental emissions in the production of ethylene. At present, a demonstration plant has been built by Siluria to demonstrate the feasibility of this technology [6].

Among the catalysts reported in literature for the OCM reaction, rare earth metal oxides are probably the most widely studied. For example, La<sub>2</sub>O<sub>3</sub>-based catalysts exhibit an excellent catalytic activity and thermal stability [7-10]. Choudhary et al. [11] studied a series of Sr-doped rare earth metal oxides (La, Ce, Pr, Ne, Sa, Eu, Ga, Dy, Er, and Yb), and they found that the Sr-doped La<sub>2</sub>O<sub>3</sub> catalysts exhibited the best catalytic performance. Baidya et al. [12] claimed that La<sub>2</sub>O<sub>3</sub> or samarium (III) oxide catalysts doped with Ca, Sr, or Ba were the most active OCM catalysts of the irreducible metal oxide catalysts. An important characteristic of

these oxides is that they have very complex structural features. For example, they interact with  $\text{CO}_2$  and  $\text{H}_2\text{O}$  from ambient air creating carbonated and hydrated species [13]. These species are also present under OCM reaction conditions. As a matter of fact in our previous study, we detected the presence of  $\text{LaOOH}$ ,  $\text{La}(\text{OH})_3$  and  $\text{La}_2\text{O}_2\text{CO}_3$  by in situ LRS. While hydroxide prevailed at low temperature, the presence of oxycarbonates started to be relevant when the reaction took place at temperatures around  $400^\circ\text{C}$ , and above  $700^\circ\text{C}$  all lanthanum species decomposed into  $\text{La}_2\text{O}_3$  [14].

In order to contribute to the development of new technologies for exploiting methane reserves, it is important to study the methodology of scaling from lab to plant conditions more deeply. Therefore, under industrial conditions, high flows should be used at relatively high temperatures. Monolithic catalysts could be a good option to study, because they provide lower pressure drop, smaller diffusion resistance and better mass and heat transfer than powder catalysts [15-17]. In a recent work we evaluated several structured catalysts (monoliths and foams) as substrates for different  $\text{Sr}/\text{La}_2\text{O}_3$  formulations [14]. We concluded that, among the catalysts studied, a cordierite monolith washcoated with  $\text{Sr}$  (5 wt.%) / $\text{La}_2\text{O}_3$  was the best option, because of its significant  $\text{C}_2$  yield and high mechanical stability. Interestingly, we found that this structured catalyst was more active than the powder one, and that at  $800^\circ\text{C}$ ,  $\text{C}_2$  yield progressively increased from around 18.0 % to 22.5% during 70 h of time-on-stream.

In this work, a systematic experimental study was designed to understand physical and chemical aspects involved in the above described behaviors. To this end, we evaluated a series of catalytic systems in which the physical effects of the honeycomb structure and the chemical interactions between the catalytic layer and cordierite were analyzed separately. A characterization of selected systems through Scanning Electron Microscopy (SEM), Energy-dispersive X-ray Spectroscopy (EDX), X-ray Photoelectron Spectroscopy (XPS) and Laser Raman Spectroscopy (LRS), were also performed to further support our hypothesis.

## **2. Experimental**

### **2.1 Structured catalyst preparation**

Honeycomb monoliths made of cordierite (Corning, 400 cpi, 0.1 mm wall thickness) were used as substrates. The cordierite composition was  $2\text{MgO}\cdot 5\text{SiO}_2\cdot 2\text{Al}_2\text{O}_3$ . The preparation method was based on the deposition of powder catalyst  $\text{Sr}(5 \text{ wt.}\%)/\text{La}_2\text{O}_3$  previously prepared by wet impregnation onto cordierite honeycomb monoliths [14]. This was accomplished by immersing the substrates during 30 s in  $20 \text{ cm}^3$  of  $\text{Sr}(5 \text{ wt.}\%)/\text{La}_2\text{O}_3$  slurry prepared in distilled water with a solid concentration of 20 wt.%. Besides, 1 wt.% of colloidal silica was added to improve adherence. After each immersion, the pieces were blown with air in order to remove the slurry excess and then they were dried at  $120^\circ\text{C}$  for 90 min. Special care was taken in the blowing step procedure, because it is important to obtain a homogeneous catalytic layer. The improvement in this preparation step resulted in a catalytic behavior slightly different from that obtained in the previous work [14],  $\text{C}_2$  selectivity being higher and methane conversion somewhat lower. This immersion-blowing-drying cycle was repeated as many times as necessary to achieve the desired catalyst loading. Then, the samples were calcined at  $850^\circ\text{C}$  during 4 h. This sample was denoted as SrLaM.

In order to study the effect of honeycomb structures on the catalytic behavior, the monolithic catalyst SrLaM was milled, and denoted as SrLaM-milled. Another powder catalyst was also prepared, by loosely mixing  $\text{Sr}(5 \text{ wt.}\%)/\text{La}_2\text{O}_3$  and milled cordierite, denoted as SrLa+M-milled. To further analyze the chemical interactions between Sr and cordierite, catalysts without lanthanum were prepared. This was done by impregnation of the monolith with a 0.47M  $\text{Sr}(\text{NO}_3)_2$  solution, reaching 5 wt.% of Sr. This catalyst was calcined at  $850^\circ\text{C}$  during 4 h and it was denoted as SrM.

## 2.2. Catalytic tests

The experiments were conducted in a fixed-bed flow quartz reactor at atmospheric pressure. The reactor design was described in a previous work [14]. The system was heated with a furnace to reach the desired temperatures. The exiting gases from the reactor were conducted through a condenser in order to eliminate  $\text{H}_2\text{O}$  from the flow. Finally, the exiting flow was measured using a gas chromatograph (GC-2014 Shimadzu) with thermal conductivity detector (TCD) equipped with two columns, Zeolite 5A and Hayesep D. The carbon balance was always higher than 97%. The catalytic tests were repeated several times over SrLaM and powder samples, showing quite reproducible results.

The reaction mixture consisted of 64 vol.% CH<sub>4</sub>, 8 vol.% O<sub>2</sub> and 28 vol.% He. The catalyst weigh/total flow ratio was 0.166 mg cm<sup>-3</sup> h. The catalysts were tested in a wide temperature range (300-800°C).

Methane conversion, C<sub>2</sub> selectivity and C<sub>2</sub> yield were calculated as follows:

Methane conversion (%) = (moles of methane reacted/moles of methane in feed)×100

C<sub>2</sub> selectivity (%) = 2(moles of C<sub>2</sub>/moles of methane reacted)×100

C<sub>2</sub> yield (%) = methane conversion (%)×C<sub>2</sub> selectivity (%)×1/100

## 2.3 Catalysts characterization

### 2.3.1. Textural Properties

N<sub>2</sub> adsorption and desorption isotherms were obtained at -196 °C with an ASAP 2020 Physisorption, Micromeritics instrument. Prior the measurement, the samples were degassed under vacuum at 250 °C for 4 h. The BET equation was used for obtaining the specific surface area, and average pore size was calculated using the Gurvich rule ( $dp$  (nm) = 4  $V_p$ .Sg<sup>-1</sup> 10<sup>3</sup>). The results were referred to powder weight in the case of Sr/La<sub>2</sub>O<sub>3</sub> and to total weight (cordierite + powder) in the case of monolithic catalyst.

### 2.3.2. X-ray Diffraction

The patterns of powder and monolithic catalysts were measured on a Shimadzu XD-D1 instrument with monochromator using Cu-Kα radiation at a scanning rate of 2 °·min<sup>-1</sup>.

### 2.3.3. Laser Raman Spectroscopy (LRS)

Raman analyses were performed in a Horiba JOBIN YVON Lab RAM HR instrument. The excitation source was the 514.5 nm line of Spectra 9000 Photometrics Ar ion laser with its power set at 30 mW.

### 2.3.4. Scanning Electron Microscopy (SEM) and Energy Dispersive Spectrometer (EDS)

The morphology of the catalytic coatings was examined with a scanning electron microscope SEM, Phenom ProX operated at an adjustable acceleration voltage range between 4.8 and 15 kV imaging and analysis mode. Pieces of different samples were observed in order to study the inner channel walls and cross-sections.

The elemental chemical analysis was performed using a Phenom ProX microscope with a fully integrated EDS detector and software. Results were obtained by the theoretical quantitative method (SEMIQ) which does not require standards. The distribution of the different elements in the catalytic layer was evaluated with the Element Identification (EID) software package and a specially designed and fully integrated Energy Dispersive Spectrometer (EDS). The apparatus was equipped with a Silicon Drift Detector Thermoelectrically cooled (LN<sub>2</sub> free). Samples were studied using a charge reduction sample holder and it was not necessary to coat them.

### 2.3.5. X-ray Photoelectron Spectroscopy

The structured and powder catalysts were characterized by means of a multi-technique system (SPECS) equipped with a dual Mg/Al X-ray source. The analyzer was PHOIBOS 150 and it was operated in the fixed analyzer transmission (FAT) mode. The pass energy was of 30 eV and the Al K $\alpha$  X-ray source was operated at 200 W and 12 kV. The XPS measurements were performed on the monolithic catalysts with an operating pressure of  $4.5 \times 10^{-9}$  torr. The spectral regions analyzed were Sr 3d, O 1s, La 3d, Mg 2p, Al 2p, Si 2p and C 1s (reference B.E. 284.6 eV) for each sample. Data treatment was performed with the XPS program (Casa Software Ltda., UK). Original spectra were fitted with peaks composed by a mixture of Gaussian and Lorentzian functions, in a 70/30 ratio. The ratio of La 3d<sub>5/2</sub> and La 3d<sub>3/2</sub> peaks area was fixed to 3:2.

In order to assure reliable results, the samples were placed into the XPS holder as shown in Figure 1. Carbon tapes were used to cover bare cordierite walls. This methodology was performed to avoid cordierite contribution to the measurement.

## 3. Results and Discussion

### 3.1. Catalytic performance

Figure 2 shows the catalytic results for different samples prepared in order to investigate the nature of the improved methane conversion and C<sub>2</sub> yield observed for structured catalyst: SrLaM, SrLaM-milled, SrLa+M-milled and Sr/La<sub>2</sub>O<sub>3</sub> powder. In Figures 2(A) and (B), it can be observed that at 800°C the SrLaM catalyst, already reported in a previous work [14], reaches methane conversion and C<sub>2</sub> selectivity values higher than the ones corresponding to

the Sr/La<sub>2</sub>O<sub>3</sub> unsupported powder. This effect was tentatively attributed to two possible factors: the monolithic structure that could impact on the catalytic behavior through a better flow distribution and, probably, improved mass transfer, and to chemical interactions between the catalyst and cordierite. In order to separate such effects, the SrLaM catalyst was milled (SrLaM-milled) and tested under reaction conditions; thus, to eliminate the contribution of the geometry structure. Methane conversion and selectivity towards C<sub>2</sub> are shown in Figures 2 (A) and (B), respectively. Conversion values are similar to those reported for SrLaM, and selectivity towards C<sub>2</sub> is significantly lower. This implies that the honeycomb geometry is a beneficial aspect which directly affects the C<sub>2</sub> selectivity. On the other hand, conversion values for SrLaM-milled are higher than the ones presented by Sr/La<sub>2</sub>O<sub>3</sub> powder, suggesting that chemical interactions between the catalytic film and cordierite material are also important.

To further assess the influence of chemical interactions, a loose mixture of Sr/La<sub>2</sub>O<sub>3</sub> powder and milled cordierite was calcined and tested in reaction. The catalytic results for this sample, SrLa+M-milled, are also shown in Figure 2. It can be observed that at 800°C, conversion values are similar to those of SrLaM and higher than Sr/La<sub>2</sub>O<sub>3</sub> unsupported powder. Again, this phenomenon suggests that chemical interactions exist between catalytic and cordierite components. Noteworthy, up to 750°C the conversions of Sr/La<sub>2</sub>O<sub>3</sub> and SrLa+M-milled are similar, but at 800°C some activation under reaction conditions seems to occur.

Figure 2(B) shows selectivity towards C<sub>2</sub> for SrLa+M-milled. In this case, selectivity values are lower than the ones of Sr/La<sub>2</sub>O<sub>3</sub> powder. This could be because the existence of milled cordierite exposed to reaction gases is higher than for SrLaM and SrLaM-milled and the contribution of Al<sub>2</sub>O<sub>3</sub> may not be beneficial. Alumina acidity could cause oxidation of methane and/or products, increasing the amount of CO and CO<sub>2</sub> generated [18].

Figure 3(A) introduces the C<sub>2</sub> yield for all catalysts. Values of C<sub>2</sub> yield rise with the increase of temperature, the higher value being at 800°C for each catalyst. It can be clearly seen that SrLaM shows the higher C<sub>2</sub> yield, 17.3%, around twofold higher than that of the Sr/La<sub>2</sub>O<sub>3</sub> powder. Then, SrLaM-milled showed a C<sub>2</sub> yield value of around 13%, SrLa+M-milled 11.5% and Sr/La<sub>2</sub>O<sub>3</sub> 9%. Noticeably, for all these samples oxygen conversion was almost complete

from 750 to 800°C. This value is in agreement with the O<sub>2</sub> conversions reported in literature at these C<sub>2</sub> yield levels [19].

In order to study the possible influence of cordierite material on the catalytic activity, a bare cordierite monolith (M) and a milled one (M-milled) were evaluated in OCM reaction. Figure 3(A) shows the C<sub>2</sub> yield for these samples, as compared with those of the other catalysts. Results obtained with the empty reactor are also included. It is shown that the C<sub>2</sub> yield follows the order: M > M-milled > empty reactor, for the latter being only 2% at 800°C. This fact indicates that the structured bare cordierite support is quite active for the OCM reaction, and again, that geometry is an important fact even with the raw material.

In addition, a cordierite monolith was impregnated with Sr (5 wt.%) to study the effect of this promoter element on cordierite oxides. This catalyst was denoted as SrM and, surprisingly, methane conversion values were satisfactorily high. At 800°C, it reached 23% methane conversion, the maximum selectivity towards C<sub>2</sub> value was 47% at 750°C and the maximum C<sub>2</sub> yield was 11% at 800°C (Fig. 3(A)). This latter value was higher than the one reported for the Sr/La<sub>2</sub>O<sub>3</sub> powder under the same reaction conditions [14]. It can be noticed that Sr may be interacting with the cordierite oxides (MgO, Al<sub>2</sub>O<sub>3</sub>, SiO<sub>2</sub>) creating oxygen vacancies that are active for OCM reaction [20-22].

Another experiment performed to study the system more deeply was a "two-way run" onto SrLaM and SrLaM-milled. Figure 3 (B) shows C<sub>2</sub> yield vs. temperature for these two catalysts. In the case of SrLaM when temperature was increased, the C<sub>2</sub> yield also increased up to 17.3% at 800°C. After one hour at 800°C, the C<sub>2</sub> yield was measured again and the value rose to 18%. Subsequently, the temperature was decreased and it could be clearly seen that at each temperature, C<sub>2</sub> yield was higher than before. This behavior was maintained up to 700°C, when C<sub>2</sub> yield was the same as before. This phenomenon was also seen in the SrLaM-milled catalytic test. The C<sub>2</sub> yield increased with temperature, being 13.2% at 800°C. After staying 1 hour at 800°C, this value raised up to 13.8%. When the temperature was decreased from 800 to 700°C, at each point C<sub>2</sub> yield was higher than before. Even though the C<sub>2</sub> yield increase was around 5%, this run was performed more than one time in these catalysts and also in several other samples (with different Sr content for example), and all the results showed the same behavior. Moreover, in our previous work [14] we found that C<sub>2</sub>

yield steeply increased from 17.3% to 22.3% after 70 h of time-on-stream at 800°C. The results of this experiment are introduced in the inset of Figure 3 (B). As those results were surprising and new, they were carefully checked and we found that they were repetitive.

At 600°C no changes in C<sub>2</sub> yield values were seen, suggesting that there exists a chemical activation of the catalyst that occurs when higher C<sub>2</sub> production is obtained at 800°C. Thus, it was concluded that the enhanced catalytic activity was due to the presence of cordierite in the catalytic system, since no C<sub>2</sub> yield increment has been reported in literature during time-on-stream tests over Sr/La<sub>2</sub>O<sub>3</sub> powders [22]. Therefore, both of these experiments are suggesting an activation of the catalyst with time under reaction conditions, and the fact that this phenomenon was also seen in the milled catalyst could be useful to conclude that this behavior is related to chemical interactions between the catalyst and cordierite.

Finally, in this section two important conclusions have been reached. The first one is that there exist some physical factors that improve the catalytic performance of SrLaM in OCM reaction. The other one is that there also exists a chemical activation that occurs when the monolithic catalyst is exposed to reaction conditions at 800°C. This latter activation could be due to the presence of cordierite components. In the following sections, these two phenomena will be studied.

### 3.2. Physical effects: Textural properties

As described above, we suggest that two factors could contribute to the improved yield observed in the monolithic catalyst: a chemical interaction between cordierite and catalyst particles (at 800°C) and physical factors. One of the most important physical parameters that can affect the catalytic behavior is BET surface area. Table 1 shows that La<sub>2</sub>O<sub>3</sub> has a surface area of 16.3 m<sup>2</sup>/g and after the impregnation of Sr and calcination, the value decreases up to 9.4 m<sup>2</sup>/g, most probably due to some plugging of the pores with Sr oxide. An important conclusion that can be drawn from the table is that the surface area of SrLaM catalyst (2.6 m<sup>2</sup>/g) is approximately a result of the addition of bare cordierite surface (0.8 m<sup>2</sup>/g) and the Sr/La<sub>2</sub>O<sub>3</sub> powder (9.4 m<sup>2</sup>/g). The SrLaM is composed of 27 wt.% of Sr/La<sub>2</sub>O<sub>3</sub> and 63 wt.% of cordierite [14], thus their contributions are 2.5 m<sup>2</sup>/g and 0.5 m<sup>2</sup>/g, respectively. Moreover, the BET value obtained for the monolithic catalyst (2.6 m<sup>2</sup>/g) is even somewhat lower than the one theoretically expected (3.0 m<sup>2</sup>/g) if we estimate this value with each contribution and

BET surface area of powder and cordierite. This fact could be proving that not only there are no improvements in surface area when the powder catalyst is incorporated into the structure, but that it also slightly decays. Moreover, after 100 h of the time-on-stream test, while  $C_2$  yield shows an important increase, the BET surface area number slightly decreases to  $2.3 \text{ m}^2/\text{g}$ . This demonstrates that the upturn in catalytic activity shown by the structured catalyst is not due to BET surface area. In the same way, changes in average pore size are not significant. Since the particle diameter does not vary from the powder to the monolithic catalyst, it is suggested that the physical parameter that could be improving the activity is the geometry of monolith. This geometry allows a better dispersion of the powder in a homogeneous film where the catalytic particles keep their identity and morphology. This distribution could also be improving the reactant flow through the catalyst making it more homogeneous than in the bulk powder thus improving mass and thermal transfer rates. In a recent work we demonstrated the absence of strong hot points along the catalytic bed when the catalyst was supported onto cordierite monoliths [14]. In this previous study the temperature profile along the LaSrM monolithic catalyst was determined under reaction conditions at  $800^\circ\text{C}$ . This was done by placing a thermocouple at different positions (four points) inside the central channel of monolith. An almost flat temperature profile was obtained, which was probably due to the low heat flux involved. As a matter of fact, the heat flux calculated from the reaction enthalpy and the observed methane conversion was only  $2.12 \text{ W}$  [14].

In regard to mass transfer, it is well known that OCM is a homogeneous/heterogeneous reaction. It has been widely studied in literature that the formation of methyl radicals occurs in the catalytic surface and their coupling to obtain  $C_2$  hydrocarbons in the gas phase [23]. Thus, when the powder catalyst was incorporated into a monolithic structure it was possible to achieve a better gas phase/catalytic surface ratio. Improving this ratio with respect to the bulk catalyst, allows reaching better OCM performances. Moreover, the fact that the  $C_2$  selectivity dropped when SrLaM was milled suggests that these mass transfer benefits of the honeycomb structure exist.

Another important property to consider is the possible change in crystallinity. However, the XRD patterns of powder catalysts ( $\text{Sr/La}_2\text{O}_3$ ), fresh monolithic sample (SrLaM) and the one

used after 100 h of reaction, do not show significant differences (See Supplementary material, Figure S1).

### 3.3. Chemical effects: Spectroscopic characterization

#### 3.3.1 Laser Raman Spectroscopy results

In order to study the possible reasons for the chemical activation of SrLaM catalyst introduced in Section 3.1, several characterization techniques were performed. Figure 4 shows Raman spectra for the SrLaM monolith, fresh sample, after the reaction test shown in Figure 1 and for the same monolith after 100 h of time-on-stream at 800°C. These samples are denoted as SrLaM-fresh, SrLaM-us and SrLaM-100, respectively.

While for the SrLaM sample only the main signals corresponding to  $\text{La}_2\text{O}_3$ ,  $\text{La}_2\text{O}_2\text{CO}_3$  and  $\text{La}(\text{OH})_3$  are evident, for the used catalysts LRS spectra become rather complex. SrLaM shows  $\text{La}(\text{OH})_3$  signals at 140, 226, 287, 343, 453 and 610  $\text{cm}^{-1}$ , and one  $\text{La}_2\text{O}_2\text{CO}_3$  band at 1072  $\text{cm}^{-1}$  [24]. At 179 and 397  $\text{cm}^{-1}$  two weak signals appeared and they are attributed to  $\text{La}_2\text{O}_3$ . SrLaM-us exhibits the same lanthanum bands as the fresh catalyst. In addition, two new signals can be observed at 682 and 848  $\text{cm}^{-1}$ . The first one was attributed to  $\text{La}_2\text{O}_2\text{CO}_3$  [25]. Mestl et al. reported a surface peroxide group signal at 846  $\text{cm}^{-1}$  in their in Situ Raman study for Sr/ $\text{La}_2\text{O}_3$  catalysts [26]. This oxygen species is believed to be one of the most active species for OCM reaction. Therefore, the band seen at 848  $\text{cm}^{-1}$  could be attributed to this active peroxide specie. Moreover, the oxide signals are clearer in this catalyst and the ones corresponding to oxycarbonate are stronger, if compared with the fresh one.

The spectrum of the catalyst exposed during 100 hours under reaction conditions, SrLaM-100, presents no significant differences from SrLaM-us. However, in the band at 450  $\text{cm}^{-1}$ , a more evident deformation can be clearly seen. This fact suggests that other components are present on the catalyst surface. It has been reported in the literature that in this region, Si-O-Si and Mg-O stretching modes could appear [27-28]. Therefore, this could be a confirmation of our chemical interaction hypothesis: when the monolithic catalyst remains at high temperature (800°C) under reaction conditions for some time, the migration of cordierite components from the structure to the catalyst film starts to be relevant. These components reach film surface, being responsible for the catalytic activity increase. It is well known that

Mg and Si are active components in the OCM reaction [29-31]. This phenomenon could also be the explanation of C<sub>2</sub> activation during the catalytic test. While after the calcination treatment (4 hours at 850°C) the interactions between catalyst and monolith take place, during the reaction at 800°C an additional activation occurs, probably because water and carbon dioxide products form carbonates and hydroxides intermediates may facilitate migration of Si and Mg from cordierite to the catalytic film. In addition, between 1400 and 1600 cm<sup>-1</sup> there are no signs of carbon deposition because no C-C bonds signals were seen.

### 3.3.2 SEM and EDX Results

In Figure 5(A) SEM and EDX results for SrLaM-us are presented. SEM micrograph clearly shows that the catalytic film is still attached to the monolith wall that establishes its satisfactory adherence and also its homogeneous morphology. As a matter of fact, if this monolith is compared with the fresh one, no significant changes are seen [14]. The graph presented in Figure 5(A) –left- shows the atomic concentration variation of different elements with the position in the monolithic catalyst (cordierite and film). If Sr atomic concentration is followed, it could be clearly seen that its concentration is almost even into cordierite and film (15 wt.%). Lanthanum concentration is roughly detectable into cordierite structure and it starts to be relevant in the active film, where its proportion is approximately 35 wt.%. Aluminum, silicon and magnesium atomic concentrations in cordierite are mostly constant, and in the active film their concentrations are lower, but they are not zero. At the surface, aluminum concentration is around 15%, silicon 20 % and magnesium 17%. These are average volumetric values due to the experiment measurement conditions. Thus, this experiment is useful to give information of the atomic concentration evolution of different species. According to this fact, it can be concluded that migration of cordierite components to the catalytic film exists and that strontium also migrates from the film to the cordierite wall. These results are in agreement with LRS results, where the lanthanum signal at 450 cm<sup>-1</sup> is distorted due to Mg or Si presence onto the surface.

The SrLaM-100 micrograph is presented in Figure 5(B). It can be clearly seen that after 100 h of time-on-stream test there were no significant changes with respect to the fresh catalyst. This further proves the excellent mechanical stability of catalytic coating. In this figure –left-, the atomic concentration variation of different components between monolithic wall and

catalytic film can also be seen. Sr and La behaviors are similar to those reported for SrLaM and SrLaM-us. Cordierite components, magnesium, aluminum and silicon, behave mostly the same as in the other structured catalysts. However, they have a significant difference: near the surface, the atomic concentration of cordierite components significantly increases. Moreover, if the surface is analyzed, it could be seen that the cordierite components concentration is quite higher in this case. In addition, if the Mg concentration evolution is analyzed, it can be observed that it does not fall significantly from the cordierite wall to the catalytic film. It may be thought that its composition remains constant onto cordierite and film. As said above, the presence of cordierite species, as Mg, Si and Al could be responsible for the C<sub>2</sub> yield improvement seen by the catalytic test. These elements could be modifying either La or Sr, generating more active sites for the OCM reaction.

In Figure 6 SEM micrographs of SrM are shown. These images were taken from a channel wall, where cordierite and some white points could be seen. Elemental composition was taken on several wall locations and a composition of around 3 wt.% Sr was obtained. However, on the white points strontium composition was higher, of around 27 wt.%. This phenomenon indicates that 3 wt.% Sr is well dispersed onto cordierite but the exceeding 2 wt.% is accumulated on the white spots. It is believed that Sr promotes basic oxides as La<sub>2</sub>O<sub>3</sub> or MgO creating oxygen vacancies that are the active sites for the OCM reaction, giving place to the satisfactorily good activity observed in Figure 2 [32].

### 3.3.3 XPS Results

Table 2 includes the surface atomic ratios between cordierite components (Si, Al and Mg) and lanthanum for SrLaM, SrLaM-us and SrLaM-100. The presence of Si, Al and Mg over the SrLaM surface is clearly demonstrated by the *cordierite component/La* ratios, which confirm what was seen by EDX experiments in previous work [14]. Noticeably, these cordierite components migrate from the monolithic structure to the catalytic surface. If SrLaM-us surface composition is analyzed, it can be clearly observed that the concentration of cordierite components increases. The atomic ratios of Si/La, Al/La and Mg/La are 1.49, 0.26 and 0.66, respectively. These values show that the migration phenomenon is improved after reaction. Moreover, when the catalyst remains under reaction conditions during 100 h (SrLaM-100), every cordierite component concentration increases except for Al. According

to these results, it can be concluded that Mg migration is higher than Si and Al. As a matter of fact, magnesium oxide is one of the most active species for OCM reaction. Therefore, when the monolithic catalyst is exposed to reaction conditions at 800°C, the migration of cordierite components is promoted. This phenomenon might be responsible for the C<sub>2</sub> yield increment due to more active sites present over the catalytic surface because of Mg. Several authors have reported the beneficial effects of Mg promoted La and La promoted Mg [33-34]. V.R. Choudhary et al. studied the La/Mg ratio in the OCM reaction and showed that this ratio affects catalyst basicity and surface area [35]. These two factors strongly influence catalytic activity.

Table 2 also shows Sr/La ratio for SrLaM, SrLaM-us, SrLaM-100. This ratio is 0.11 for the fresh catalyst, 0.46 for the one used in reaction and 0.52 for the catalyst used 100 h under reaction conditions. This result denotes that Sr migration to the catalytic surface is also increased when OCM reaction takes place. This component promotes lattice oxides creating oxygen vacancies that are the active sites in the OCM reaction.

Figure 7 shows the XPS spectra of O 1s for SrLaM-us and SrLaM-100. In the SrLaM-us spectrum three signals at 528.4, 531.5 and 533.2 eV can be observed. The signal at lower binding energy could be assigned to lattice oxygen. At 531.5 eV there appear peroxide ion (O<sup>-</sup>), CO<sub>3</sub><sup>2-</sup> and OH<sup>-</sup> oxygen species. This signal could be formed by a contribution of these three components as it is shown in Figure 7. Therefore, the existence of this signal confirms what was seen by LRS results, the presence of lanthanum oxycarbonate, lanthanum hydroxide and this OCM active oxygen species (O<sup>-</sup>). The latter signal, at 533.2 eV, could be assigned to superoxide ions, the most active oxygen species for OCM [36]. It is believed that electron deficient species of oxygen are the most active ones for the OCM reaction. They were supposed to be responsible for hydrogen abstraction from the methane molecule to form methyl radicals, which is the limiting reaction step [37]. In the SrLaM-100 spectrum no significant differences with SrLaM-us were observed.

The O 1s spectrum of the SrLaM fresh catalyst was reported in a previous work [14], where it was observed that the lattice oxygen contribution was higher than for these used catalysts, and no existence of superoxide species was observed. The higher lattice concentration was attributed to the presence of cordierite oxides (MgO, Al<sub>2</sub>O<sub>3</sub>, SiO<sub>2</sub>) onto catalytic surface. In

the used catalysts, this lattice oxygen species concentration is lower and the superoxide signal appears which, is in agreement with LRS results. When the catalyst is exposed to reaction conditions at 800°C, OCM active oxygen species ( $O^-$  and  $O^{2-}$ ) start to be relevant. Thus, this phenomenon could explain the increase of the  $C_2$  yield during 70 h of reaction, because more active sites are generated during this time.

The increase of active sites under reaction conditions could be due to the continuous formation and decomposition of carbonate, oxycarbonate and hydroxide species. These species, at 800°C are extremely unstable, and they decompose into the oxides, but the presence of  $CO_2$  and  $H_2O$  during reaction could be continuously promoting their formation. This phenomenon could be responsible for promoting the migration of cordierite components to the catalytic film, and also Sr migration to the surface. The presence of these components into the film could be related with the increment of  $O^-$  and  $O^{2-}$ , which are active oxygen species for the OCM reaction.

The facts described in the above paragraphs may be the reasons for the increase of the  $C_2$  yield during reaction conditions. And this also confirms the existence of chemical interactions between cordierite and catalytic film components, hypothesis suggested in a previous work [14].

### **3.4. Relevant features about the OCM reaction on powder and monolithic catalyst.**

Previously mentioned, it is well known that OCM is a homogeneous/heterogeneous reaction. It has been widely studied in literature that the formation of methyl radicals occurs in the catalytic surface and their coupling to obtain  $C_2$  hydrocarbons in the gas phase [23]. Thus, when the powder catalyst was impregnated into monolithic structure it was possible to achieve a better gas phase/catalytic surface ratio. Improving this ratio with respect to the bulk catalyst, allows reaching better OCM performances. In order to gain insight into the beneficial effect of the incorporation of the  $Sr/La_2O_3$  powder onto cordierite monoliths structures on the catalytic behavior for OCM reaction, this effect has been systematically studied through the preparation of different powder and monolithic formulations. One of the main causes of the observed effect may be the even flow distribution which probably results

in improved mass transfer inside the monolith channels, thus increasing the overall reaction rate.

The efficiency of mass transport processes in monolithic catalysts depends on the thickness of the catalytic layer and the homogeneity of the gaseous flow, among others variables. When the catalytic film is thicker, the diffusion resistance is higher. In our monolithic catalyst, the thickness of the film was only about 30  $\mu\text{m}$ . Thus we may think that it does not state an additional mass transfer resistance, as compared with individual particles. In the same vein, in a recent work Merino et al. [38] reported that below 50  $\mu\text{m}$  there is no additional diffusion resistance for the Fischer-Tropsch reaction on a Co,Re/Al<sub>2</sub>O<sub>3</sub> catalytic layer deposited on a metallic monolith. On the other hand, the gaseous flow is more homogeneous in the channels of the monolith than in a powder catalytic bed, with the additional advantage of a lower pressure drop, which results in better contact between reactants and catalytic surface, thus increasing the overall reaction rate. A deep discussion of these aspects can be found in Moulijn et al. [39].

In this work, it has also been demonstrated that chemical interactions between the catalytic film and the cordierite material is another cause of the improved conversion and C<sub>2</sub> yield. These chemical interactions are originated in the incorporation of Mg and Si into the Sr/La<sub>2</sub>O<sub>3</sub> film, phenomenon that was further increased under reaction conditions at 800°C. By means of EDX, the migration of the cordierite components to the catalytic film was corroborated. The presence of peroxide species onto the surface of the monolithic catalyst exposed to reaction conditions was first seen by LRS. This species along with superoxide species were confirmed by the XPS technique. The migration of Si, Mg and Al was also established when the catalysts were used in OCM reaction. It could be concluded that when the catalyst is exposed to reaction conditions at 800°C, carbonate, oxycarbonate and hydroxide species are continuously being created and decomposing. This phenomenon is suggested to be the one that promotes cordierite components migration to the catalytic film and this generates more peroxide and superoxide species that are the catalytic active sites for OCM reaction. For a lower temperature (600°C), the increase in the C<sub>2</sub> yield was not observed during time-on-stream experiment, probably because at this temperature the mobility of the species present in the monolithic structure is not high enough and the catalytic

layer is not enriched with Si, Mg and Al as it occurs at 800°C, which was demonstrated by XPS and EDX characterization.

## 4. Conclusions

In this work we have shown that when powder Sr/La<sub>2</sub>O<sub>3</sub> catalysts are deposited on the walls of cordierite monoliths, an important increase in both, methane conversion and C<sub>2</sub> yield, takes place. We suggest that the improved catalytic behavior is due to a combination of physical and chemical factors, consisting in a) a more homogeneous flow provided by the monolithic structure which results in a better contact between reactant and catalyst surface, which in turn results in an increase of the overall reaction rate, and b) the incorporation of Mg and Si from the cordierite material into the Sr/La<sub>2</sub>O<sub>3</sub> film, phenomenon that is further increased under reaction conditions at 800°C. This phenomenon does not take place at lower temperatures (600°C) probably due to the lower mobility of the species present in the cordierite. To reach these conclusions, we performed a systematic study in which several structured formulations were catalytically evaluated and characterized using different techniques (EDX, XRD, BET, XPS, LRS) which helped us to rationalize the experimental observations.

## 5. Acknowledgments

The authors wish to acknowledge the financial support received from UNL, ANPCyT and CONICET. They are also grateful to ANPCyT for PME Grants to finance the purchase of the characterization equipment. Thanks are given to María Fernanda Mori for the XPS measurements.

## References

- [1] J. Alper, *The Changing Landscape of Hydrocarbon Feedstocks for Chemical Production: Implications for Catalysis*, The National Academies of Sciences - Engineering - Medicine, 2016.
- [2] The Oxford Institute for Energy Studies, University of OXFORD, *Unconventional Gas in Argentina*, October 2016.
- [3] A. Farsi, S.S. Mansouri, *Arabian J. of Chem.* 9 (2016) 28 – 34.
- [4] G.S. Lane, E.E. Wolf, *J. Catal.* 113 (1988)144-163.
- [5] E.E. Miró, Z. Kalenik, J. Santamaría, E.E. Wolf, *Catal. Today* 6 (1990) 511-518.
- [6] A. Galadima, O. Muraza, *J. Ind. Eng. Chem.* 37 (2016) 1 - 13.
- [7] K. Otsuka, K. Jinno, A. Morikawa, *J. Catal.* 100 (1986) 353–359.
- [8] T. Jiang, J. J. Song, M. F. Huo, N. T. Yang, J. W. Liu, J. Zhang, Y. H. Sun, Y. Zhu, *RSC Adv.* 6 (2016) 34872–34876.
- [9] R. Ghose, H.T. Hwang, A. Varma, *Appl. Catal. A: Gen.* 472 (2014) 39-46.
- [10] R. Ghose, H.T. Hwang, A. Varma, *Appl. Catal. A: Gen.* 452 (2014) 147-154.
- [11] V. R. Choudhary, S. A. R. Mulla, V. H. Rane, *J. Chem. Technol. Biotechnol.* 71 (1998) 167–172.
- [12] T. Baidya, N. Vegten, R. Verel, Y. Jiang, M. Yulikov, T. Kohn, G.Jeschke, A. Baiker, *J. Catal.* 281 (2011) 241–253.
- [13] G. Adachi, N. Imanaka, Z.C. Kang, *Binary Rare Earth Oxides*, Kluwer Academic Publishers, U.S., 2004.
- [14] B.M. Sollier, L.E. Gomez, A.V. Boix, E.E. Miró, *Appl. Catal. A: Gen.* 532 (2017) 65 - 76.
- [15] G. Groppi, E. Tronconi, *Chem. Eng. Sci.* 55 (2000) 2161 - 2117.
- [16] A. Cybulski, J.A. Moulijn, *Catal. Reviews: Sci. and Eng.* 36 (2) (1994) 179 - 270.
- [17] P. Avila, M. Montes, E.E. Miró, *Chem. Eng. J.* 109 (2005) 11-36.
- [18] R. Mariscal, J. Soria, M.A. Peña, J.L.G. Fierro, *Appl. Catal. A: Gen.* 111 (1994) 79 - 97.
- [19] P.N. Kechagiopoulos, L. Olivier, C. Daniel, A.C. Van Veen, J.W. Thybaut, G.B. Marin, C. Mirodatos, in: N. Kanellopoulos, *Small-Scale Gas to Liquid Fuel Synthesis*, Taylor & Francis Group, Florida U.S., 2015, pp. 227-261.
- [20] G. Gayco, D. Wolf, E.V. Kondratenko, M. Baerns, *J. Catal.* 178 (1998) 441 - 449.
- [21] U. Zavyalova, M. Holena, R. Schlogl, M. Baerns, *ChemCatChem* 3 (2011) 1935 - 1947.

- [22] E.V. Kondratenko, M. Schlüter, M. Baerns, D. Linke, M. Holena, *Catal. Sci. Technol.* 5 (2015) 1668-1677.
- [23] E.E. Wolf, *Methane conversion by oxydative process: Fundamental and Engineering Aspects*, Van Nostrand Reinold Catalysis Series, Springer Science + Business Media LCC, New York U.S., 1992.
- [24] A.M. Jastrzebska, E. Karwowska, A.R. Olszyna, A. Kunicki, *Surf. Coat. Technol.* 271 (2015) 225 - 233.
- [25] S.I. Boldish, W.B. White, *Spectrochim. Acta Part A: Mol. Spectrosc.* 35 (1979) 1235 - 1242.
- [26] G. Mestl, H. Knözinger, J.H. Lunsford, *Ber. Bunsenges, Phys. Chem.* 97 (1993) 319 - 321.
- [27] V. Stefov, Z. Abdija, M. Najdoski, V. Koleva, V.M. Petrusovski, T. Runcevski, R.E. Dinnebier, B. Soptrajanov, *Vibrational Spectrosc.*, 68 (2013) 122 - 128.
- [28] A. El khalfia, E. Ech-chamikha, Y. Ijdiyaoua, M. Azizana, A. Essaftia, L. Nkhailia, A.E. Kissania, E. Tomasella, *Vibrational Spectrosc.* 89 (2017) 44 - 48.
- [29] P. Schwach, W. Frandsen, M.G. Willinger, R. Schlögl, A. Trunschke, *J. Catal.* 329 (2015) 560-573.
- [30] P. Schwach, N. Hamilton, M. Eichelbaum, L. Thum, T. Lunkenbein, R. Schlögl, A. Trunschke, *J. Catal.* 329 (2015) 574-587.
- [31] N. Hiyoshi, K. Sato, *Fuel Processing Tech.* 151 (2016) 148 - 154.
- [32] Z. Kalenik, E. E. Wolf., *Catal. Today* 13 (1992) 255 - 264.
- [33] Z. Gao, Y. Shi, *J. Natural Gas Chem.* 19 (2010) 173 - 178.
- [34] V.R. Choudhary, S.T. Chaudhari, A.M. Rajput, V.H. Rane, *J. Chem. Soc. Chem. Commun.* 9 (1989) 555-556.
- [35] V.R. Choudhary, V.H. Rane, S.T. Chaudhari, *Fuel* 79 (2000) 1487 - 1491.
- [36] M.S. Islam, D.J. Ilett, S.C. Parker, *J. Phys. Chem.* 98 (1994) 9637-9641.
- [37] M.C. Alvarez-Galvan, N. Mota, M. Ojeda, S. Rojas, R.M. Navarro, J.L.G. Fierro, *Catal. Today* 171 (2011) 15 - 23.
- [38] D. Merino, O. Sanz, M. Montes, *Chem. Eng. J.* 327 (2017) 1033-1042.
- [39] J.A Moulijn, F. Kapteijn, *Current Opinion in Chem. Eng.* 2 (2013) 346–353.

**Table 1.** Textural properties. N<sub>2</sub> adsorption and desorption

<b>Catalysts</b>	<b>Sg (m<sup>2</sup>g<sup>-1</sup>) BET</b>	<b>Total pore volume<sup>c</sup> (cm<sup>3</sup>g<sup>-1</sup>)</b>	<b>Average pore size (nm)<sup>d</sup></b>
5Sr/La <sub>2</sub> O <sub>3</sub>	9.4	17·10 <sup>-3</sup>	7.2
SrLaM <sup>a</sup>	2.6	2.6·10 <sup>-3</sup>	4.0
SrLaM <sup>b</sup>	2.3	3.5·10 <sup>-3</sup>	6.1
Cordierite	0.8		
La <sub>2</sub> O <sub>3</sub>	16.3		

<sup>a</sup> Fresh sample.

<sup>b</sup> Used sample (after reaction experiment)

<sup>c</sup> Total pore volume measured at P/P<sub>0</sub>=0.98

<sup>d</sup> Calculated from Gurvich rule:  $dp \text{ (nm)} = 4 V_p S_g^{-1} 10^3$

**Table 2.** Surface atomic ratios from XPS measurements.

<b>Catalyst *</b>	<b>Si/La</b>	<b>Al/La</b>	<b>Mg/La</b>	<b>Sr/La</b>
SrLaM	0.62	0.06	0.03	0.11
SrLaM-us	1.49	0.26	0.66	0.46
SrLaM-100	2.02	0.26	1.05	0.52

\*Analyzed area as shown in Figure 1.

## Figure legends

**Figure 1.** XPS experiment measurements.

**Figure 2.** Catalytic test results of Sr/La<sub>2</sub>O<sub>3</sub> powder, SrLaM, SrLaM-milled and SrLa+M-milled. (A) Methane conversion vs. Temperature, and (B) C<sub>2</sub> Selectivity vs. Temperature. (Reaction conditions: w/F = 0.166 mg cm<sup>-3</sup> h, flow composition: 64 vol.% CH<sub>4</sub>, 8 vol.% O<sub>2</sub> and 28 vol.% He)

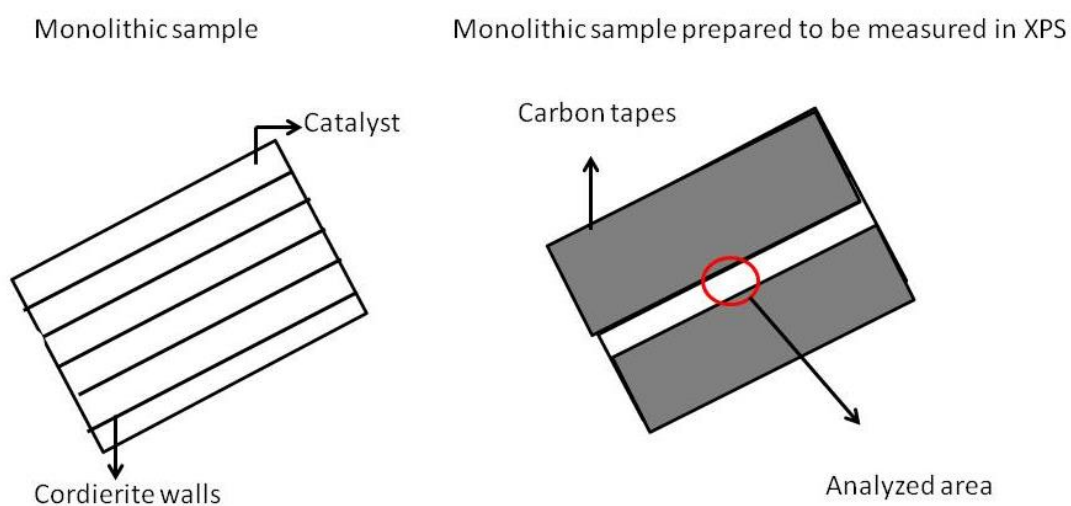
**Figure 3.** C<sub>2</sub> yield of: (A) all catalysts; (B) SrLaM and SrLaM-milled, increasing and decreasing temperature. In the inset of (B): variation of C<sub>2</sub> yield with time-on-stream for SrLaM catalyst at 800 °C and 600 °C. (Reaction conditions: w/F = 0.166 mg cm<sup>-3</sup> h, flow composition: 64 vol.% CH<sub>4</sub>, 8 vol.% O<sub>2</sub> and 28 vol.% He)

**Figure 4.** Raman spectra of SrLaM, SrLaM-us, SrLaM-100. Species: (■) La(OH)<sub>3</sub>, (▣) La<sub>2</sub>O<sub>2</sub>CO<sub>3</sub>, (■) La<sub>2</sub>O<sub>3</sub> and (\*) O<sup>-</sup>.

**Figure 5.** SEM and linear mapping onto: (A) SrLaM-us and (B) SrLaM-100.

**Figure 6.** SEM micrograph and elemental mapping onto SrM. Micrograph image from monolith walls.

**Figure 7.** XPS spectra of O 1s region from SrLaM-us and SrLaM-100.

**Figures****Figure 1.** XPS experiment measurements.

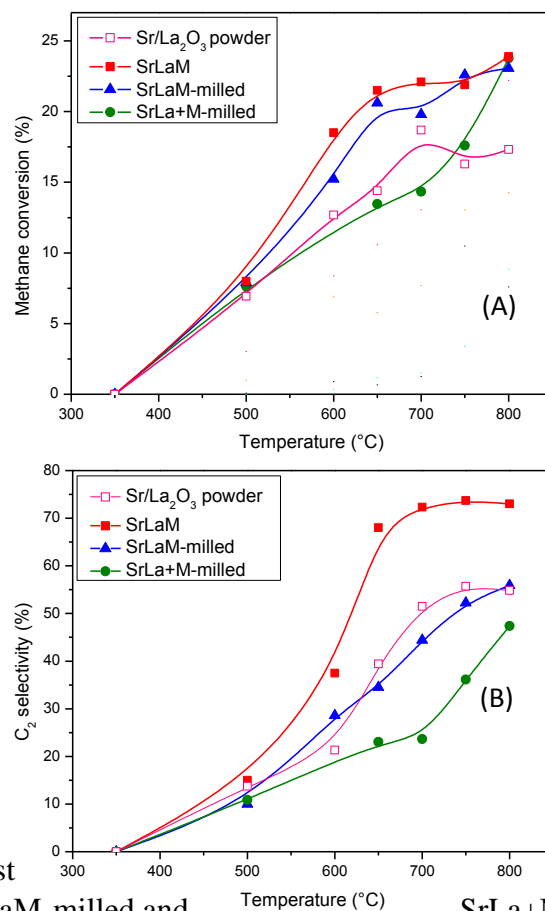


**Figure 2.** Catalytic test results of Sr/La<sub>2</sub>O<sub>3</sub> powder, SrLaM, SrLaM-milled and SrLa+M-milled. (A) Methane conversion vs. Temperature, and (B) C<sub>2</sub> Selectivity vs. Temperature. (Reaction conditions: w/F = 0.166 mg cm<sup>-3</sup> h, flow composition: 64 vol.% CH<sub>4</sub>, 8 vol.% O<sub>2</sub> and 28 vol.% He)

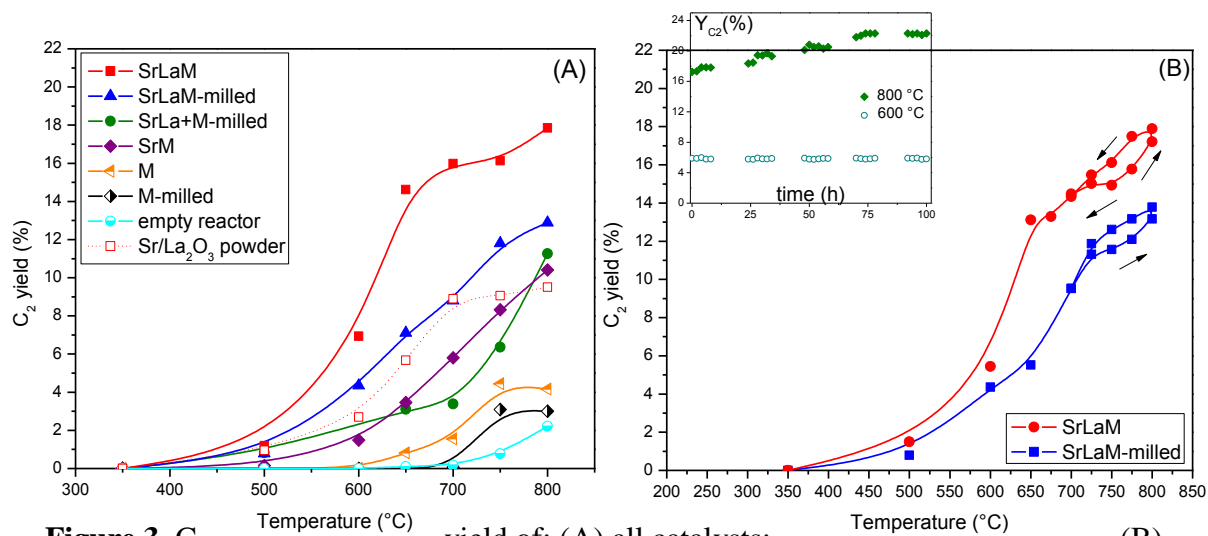


**Figure 3.** C<sub>2</sub> yield of: (A) all catalysts; (B) SrLaM and SrLaM-milled, increasing and decreasing temperature. In the inset of (B): variation of C<sub>2</sub> yield with time-on-stream for SrLaM catalyst at 800 °C and 600 °C. (Reaction conditions: w/F = 0.166 mg cm<sup>-3</sup> h, flow composition: 64 vol.% CH<sub>4</sub>, 8 vol.% O<sub>2</sub> and 28 vol.% He)

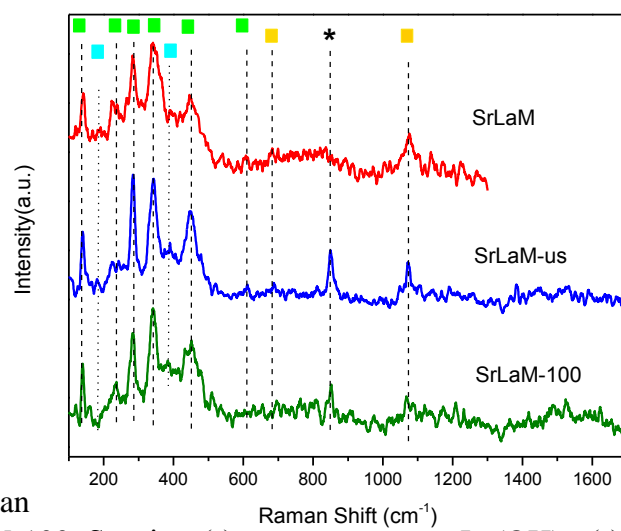


**Figure 4.** Raman spectra of SrLaM, SrLaM-us, SrLaM-100. Species: (■)  $\text{La}(\text{OH})_3$ , (■)  $\text{La}_2\text{O}_2\text{CO}_3$ , (■)  $\text{La}_2\text{O}_3$  and (\*)  $\text{O}^{2-}$ .

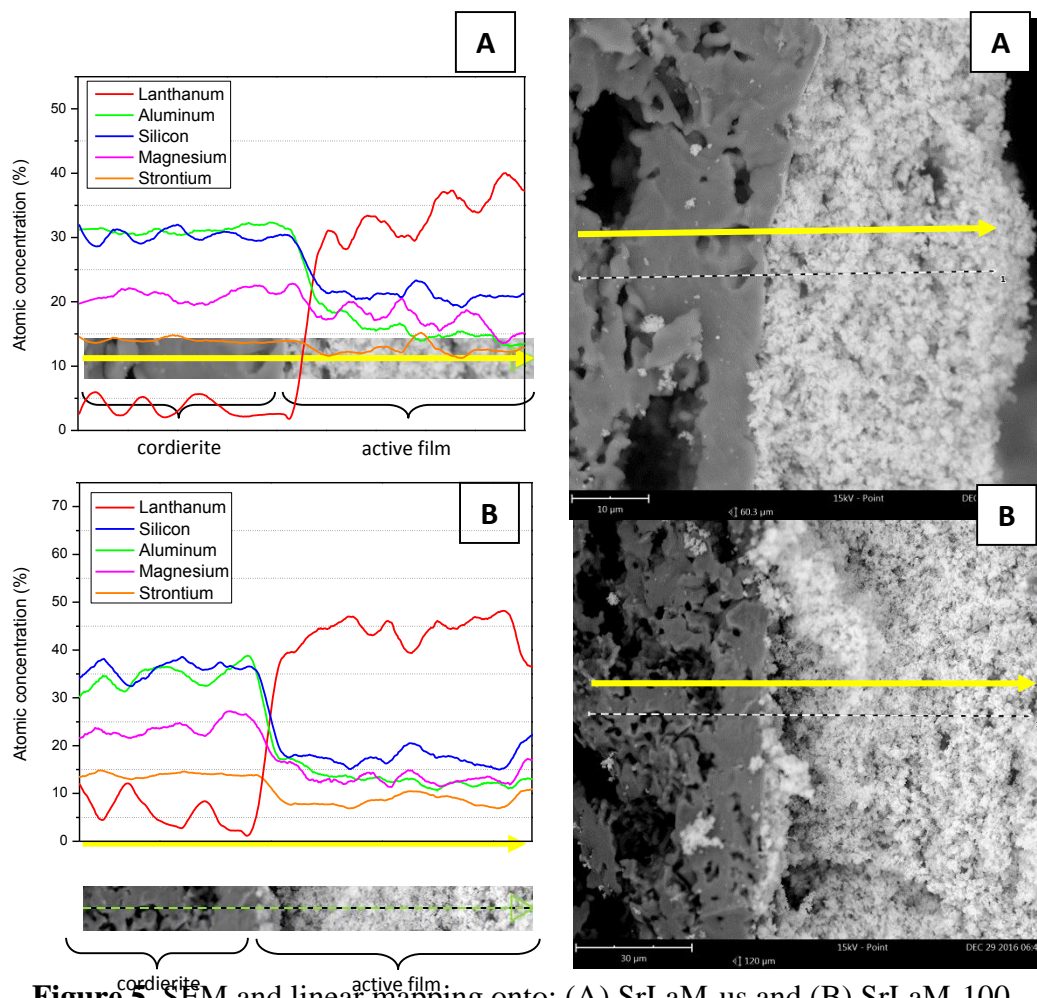


**Figure 3.** SEM and linear mapping onto: (A) SrLaM-us and (B) SrLaM-100.

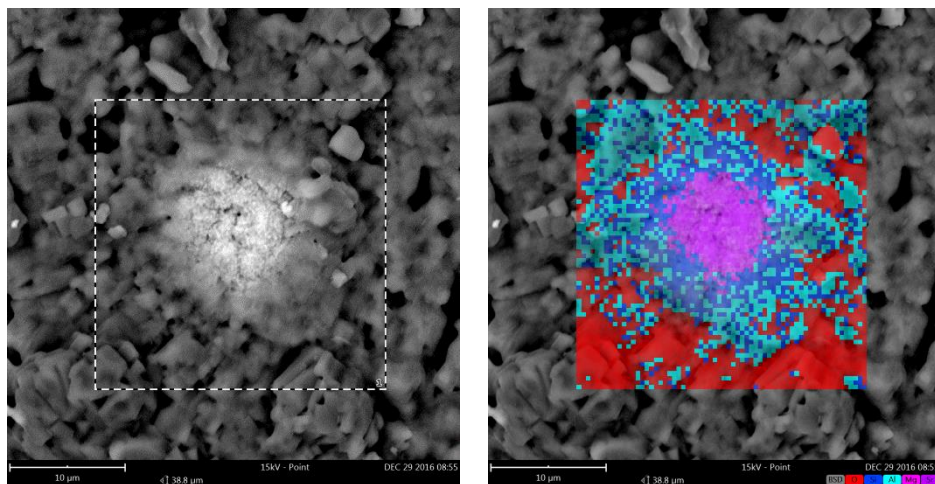


**Figure 6.** SEM micrograph and elemental mapping onto SrM. Micrograph image from monolith walls.

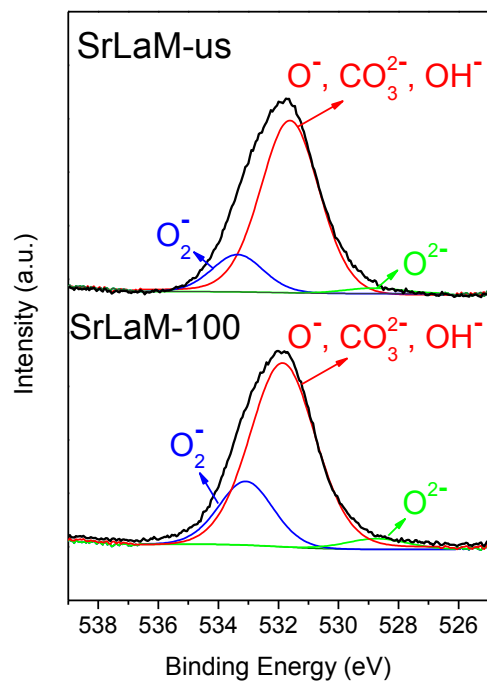


**Figure 7.** XPS spectra of O 1s region from SrLaM-us and SrLaM-100.